Thermal spin torques in magnetic insulators

H. Yu, S. D. Brechet, P. Che, F. A. Vetro, M. Collet, S. Tu, Y. G. Zhang, Y. Zhang, T. Stueckler, L. Wang, H. Cui, D. Wang, C. Zhao, P. Bortolotti, A. Anane, J-Ph. Ansermet, and W. Zhao

Phys. Rev. B **95**, 104432 — Published 23 March 2017
DOI: 10.1103/PhysRevB.95.104432

Thermal spin torques in magnetic insulators

H. Yu,[1,2,*] S. D. Brechet,[2] P. Che,[1,2] F. A. Vetro,[2] M. Collet,[3] S. Tu,[1,2]
Y. G. Zhang,[1] Y. Zhang,[1] T. Stueckler,[1] L. Wang,[1,4] H. Cui,[4] D. Wang,[4]
C. Zhao,[4] P. Bortolotti,[3] A. Anane,[3] J-Ph. Ansermet,[2,†] and W. Zhao[1]

[1]*Fert Beijing Research Institute, School of Electrical and Information Engineering, BDBC, Beihang University, China*
[2]*Institute of Physics, station 3, Ecole Polytechnique Fédérale de Lausanne, 1015 Lausanne-EPFL, Switzerland*
[3]*Unité Mixte de Physique CNRS, Thales, Univ. Paris Sud, Université Paris-Saclay, 91767 Palaiseau, France*
[4]*Institute of Microelectronics, Chinese Academy of Sciences, Beijing 100029, China*

(Dated: March 3, 2017)

The damping of spin waves transmitted through a two-port magnonic device implemented on a YIG thin film is shown to be proportional to the temperature gradient imposed on the device. The sign of the damping depends on the relative orientation of the magnetic field, the wave vector and the temperature gradient. The observations are accounted for qualitatively and quantitatively by using an extension of the variational principle that leads to the Landau-Lifshitz equation. All parameters of the model can be obtained by independent measurements.

The discovery of giant magneto-resistance (GMR) revolutionized information storage technology [1, 2] and the spin-transfer torque (STT), predicted two decades ago by Slonczewski [3] and Berger [4], may reshape once again the magnetic memory industry [5]. The concept of a heat-driven spin torque, or thermal spin-transfer torque (TST), has been suggested [6–8] and opened the world of spin caloritronics. Magnetic insulators are ideal for studying the fundamentals of spin caloritronics, because they are free of the effect of heat on charge transport. Here, we demonstrate that a spin torque can be induced in magnetic insulators by applying a thermal gradient. The effect is not linked to spin-dependent transport at interfaces since we observe a heat-driven contribution to damping of magnetization waves on a millimeter scale. We show that by adding to $\boldsymbol{M}(\boldsymbol{r})$ the bound magnetic current $(\boldsymbol{\nabla}\times\boldsymbol{M})$ as state variable, the variational principle that yields the Landau-Lifshitz equation predicts the presence of a thermal spin torque, from which we derive an expression for spin currents in insulators. Our experiments verify the key predictions of this model. Thermodynamics can predict a link between heat and magnetization, but cannot determine the strength of the effect [9].

Spin caloritronics studies the interplay of spin, charge and heat transport [10]. As the spin-dependence of the electrical conductivity proved to be important since it gives rise to GMR, the spin-dependence of other transport parameters has been investigated, such as that of the Seebeck [11] and Peltier coefficients. [12] The combination of heat with spin and charge transport gained widespread attention owing to studies of the spin Seebeck effect [13, 14]. The STT effect which uses a spin-polarised electrical current has shown promising applications, e.g. in magnetic memories (STT-MRAM). It was already established that heat flowing through a ferromagnetic metal can

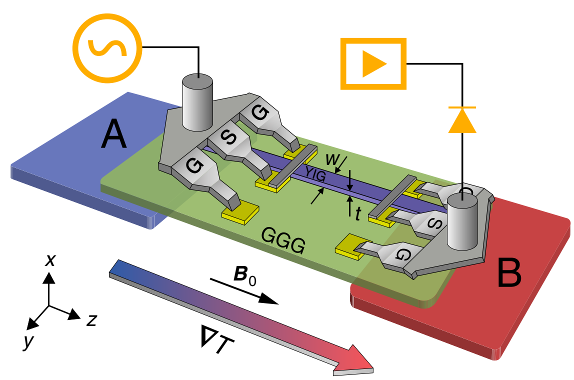

FIG. 1. Spin wave propagation under a thermal gradient. 4.8 mm-long YIG strip fabricated on GGG substrate, width $w = 100\,\mu$m, thickness $t = 20$ nm, 10 nm-thick Cu contact connected to Au electrodes, microprobes for both excitation and detection, Peltier elements A and B heat sunk by copper blocks (not shown).

generate a diffusive spin current [15] which induces a spin torque when flowing through a magnetic nanostructure [6]. Experimentally, this effect was studied in Co/Cu/Co spin valve nanowires by observing the change in the switching field of magnetisation due to a local thermal gradient [7]. It was later showed that heat couples to magnetisation dynamics. [16–18] The effect of heat on magnetization was also found in magnetic tunnel junctions [19] and metallic spin valves [20]. Slonczewski predicted that a spin-transfer torque induced by thermal magnons could be more efficient than the usual electrically-induced spin torques [8]. Combining TST and STT might further decrease the write-current magnitude of MRAMs [21].

A 20 nm-thick yttrium iron garnet (YIG) film was grown on gadolinium gallium garnet (GGG) substrate using pulsed laser deposition (PLD). Details of the growth condition and magnetic properties of the thin YIG layer can be found in Ref. [22].

Figure 1 shows the experimental principle of the measurement. Using inductively coupled plasma etching and photolithography, a YIG strip 100 μm wide and 4.8 mm long was prepared. The ends were designed with a 45° angle in order to avoid spin wave reflection. Following the etching process, a 10 nm-thick copper or platinum bar was deposited on top of the YIG strip by electron beam evaporation. This bar is connected to two large Au electrodes. These electrodes are designed for contact with a ground-signal-ground microprobe. The magnetic field is applied along the YIG strip, and spin waves are excited by one microprobe and detected by another. Alternatively, a micro-coil [23] was used for excitation. Excitation and detection are 800 μm apart. The results were obtained with contacts made of Pt with a Ta seed layer. The resonance frequency could be tuned from 4 GHz up to 10 GHz. Lock-in detection with field modulation was used. The thermal gradient was generated by two Peltier elements and defined as $\nabla T = (T_\mathrm{B} - T_\mathrm{A})/l$ with $l = 5$ mm being the distance between the Peltier elements. Using an infrared camera, we verified that the temperature changed linearly at the location of the sample.

As shown in Fig. 2, the linewidth changes linearly with temperature gradient. Furthermore, the slope changes sign when the field is reverse or when the propagation direction is reverse. For the latter case, we had to move the sample and this caused a change in the linewidth of 0.03 mT when the sample was at a uniform temperature. In Fig. 2, we translated all data points by this amount when the sample was flipped.

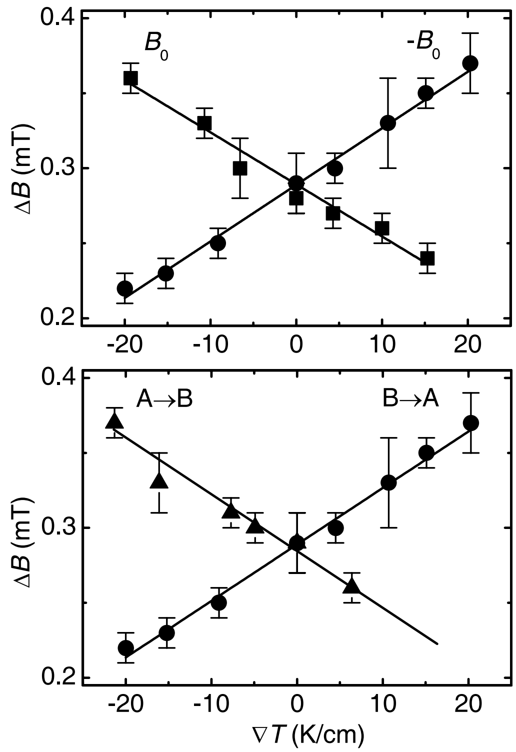

FIG. 2. Linewidth of the ferromagnetic resonance spectra at 4.2 GHz, as a function of temperature gradient. The slope changes sign upon flipping the field (top) or flipping the direction of propagation at fixed field orientation (bottom). A→B data are translated by 0.03 mT.

We can account for the observed effect of a temperature gradient on spin wave transmission by a model based on an extension of the variation principle which yields the well-known Landau-Lifshitz-Gilbert (LLG) equation [24]. In the presence of an applied thermal gradient $\boldsymbol{\nabla} T$, the LLG equation for the time evolution of the magnetisation $\boldsymbol{M}$ contains a thermal spin torque term, i.e.

$$\dot{\boldsymbol{M}} = \gamma\, \boldsymbol{M} \times \boldsymbol{B}_\mathrm{eff} + \frac{\alpha}{M_S}\, \boldsymbol{M} \times \dot{\boldsymbol{M}} + \boldsymbol{\tau}_\mathrm{TST} \qquad (1)$$

where $\gamma < 0$ is the gyromagnetic ratio, α is the magnetic damping parameter and M_S is the saturation magnetization. The effective magnetic field

$\boldsymbol{B}_{\text{eff}}$ is composed of the external field $\boldsymbol{B}_0$, the demagnetising field $\boldsymbol{B}_{\text{dem}}$, the anisotropy field $\boldsymbol{B}_{\text{ani}}$ and the microwave excitation field $\boldsymbol{b}$ induced by the microwave antenna. The torque $\boldsymbol{\tau}_{\text{TST}}$ can be expressed as,

$$\boldsymbol{\tau}_{\text{TST}} = \alpha_{\text{TST}} \frac{\omega}{|\gamma|} \boldsymbol{M} \times (\boldsymbol{M} \times \boldsymbol{m}) \tag{2}$$

where the effective thermal spin torque damping coefficient α_{TST} can be written as,

$$\alpha_{\text{TST}} = -\frac{\omega_{\text{M}}}{\omega} \frac{k_{\text{T}}}{k} \tag{3}$$

Here, ω corresponds to the microwave frequency and $\boldsymbol{m}$ is the out-of-equilibrium component of the magnetization for a mode of wave number k. In this work, we provide a quantitative expression for the thermal wave vector k_{T} with no adjustable parameter:

$$\boldsymbol{k}_{\text{T}} = \frac{\omega - \omega_0}{\omega_{\text{M}}} \left| \frac{1}{M_{\text{S}}} \frac{dM_{\text{S}}}{dT} \right| \boldsymbol{\nabla} T \tag{4}$$

where $\omega_0 = -\gamma B_0$ and $\omega_{\text{M}} = -\gamma M_{\text{S}}$. The lengthy derivation of the above equations are given in the supplementary material [25]. The effective damping parameter α_{eff} is the sum of the Gilbert damping parameter α and the thermal spin torque damping parameter α_{TST}. The observed spin-wave spectral line width is therefore given by [25],

$$\Delta B = \Delta B_0 + \frac{2}{\sqrt{3}} \alpha \left| \frac{\omega_{\text{K}}}{\gamma} \right| - \frac{2}{\sqrt{3}} \left| \frac{\omega_{\text{K}} - \omega_0}{\gamma} \right| \left| \frac{1}{M_{\text{S}}} \frac{dM_{\text{S}}}{dT} \right| \frac{1}{k} \nabla T \tag{5}$$

where ω_{K} is the resonance frequency, given by the Kittel formula [25].

Thus, our model predicts that the thermal spin torque changes sign under reversal of either the temperature gradient, the propagation direction or the applied magnetic field (Fig. 2). Initially, we varied the applied thermal gradient and observed a linear change in the spin-wave spectral linewidth for one orientation of the field. This linear dependence is consistent with Eq. (5). Clearly, when the thermal gradient changes sign, the linewidth changes from a broadening to a narrowing with respect to its value in the isothermal condition. It must be noted that the temperature has hardly any influence on the linewidth [25]. The dependence of linewidth with thermal gradient changes sign when the magnetic field is reversed (Fig. 2, top). This can be understood as follows. If ω changes sign because B is reversed, then k must change sign also if we want propagation to be maintained in the same orientation [25]. Therefore, according to Eq. (5), the slope of the linewidth plotted vs. temperature gradient must change sign when the magnetic field is reversed, as confirmed by Fig. 2 (top). Furthermore, if we swap the excitation and the detection, i.e. we reverse the spin wave vector $\boldsymbol{k}$, then we observe that the thermal spin torque effect is also reversed, as shown in Fig. 2 (bottom), which is consistent with the line width being proportional to $1/k$ (Eq. (5)).

We now investigate the frequency dependence of linewidth variation. The upper part of Fig. 3 shows the linewidth changes with frequencies from 4.7 GHz up to 9.7 GHz using a microprobe for excitation. We ran a High Frequency Electromagnetic Field Simulation (HFSS) taking into account the dimensions of the microprobe and acquired the field distribution at the injection area. We then used Fourier transformation to obtain the k space distribution [25]. Thus, we found that the most prominent excitation has a wave vector around 100 rad/cm, and that there are some higher order modes with much lower intensities. The lower part of Fig. 3 shows the frequency dependence of linewidth measured using the microcoil for excitation. According to the results from HFSS, we found that the dominant wave vector k of excitation is much smaller, namely 35 rad/cm. The slope of the frequency dependence is proportional to the effective damping parameter. We can observe that the change of the slope is more significant for microcoil excitation than that for microprobe excitation. This can be understood from Eq. (3) where the thermal spin torque induced damping parameter is inversely proportional to the spin-wave wave vector. We can account for the data using the k values deduced from the HFSS calculation. We take the temperature dependence of the saturation magnetisation to be $\left| \frac{1}{M_{\text{S}}} \frac{dM_{\text{S}}}{dT} \right| = 3.8 \times 10^{-3}$ K^{-1} based on reference [16] and confirmed by isothermal measurements of saturation magnetization [25]. In the lower part of Fig. 3, we fit the data based on Eq. (5), using the damping parameter $\alpha = 6.30 \times 10^{-4}$ deduced from the data taken without any thermal gradient. This smaller value could be due to the fact that when using the microcoil excitation, the detection was done using a Pt bar whereas a Cu bar was used when taking data with the microprobe excitation. According to Ref. [18], the growth of Pt on YIG may introduce an increase of damping. In summary, the various data presented in Fig. 3 can be accounted for quantitatively with parameters that are all determined by independent measurements.

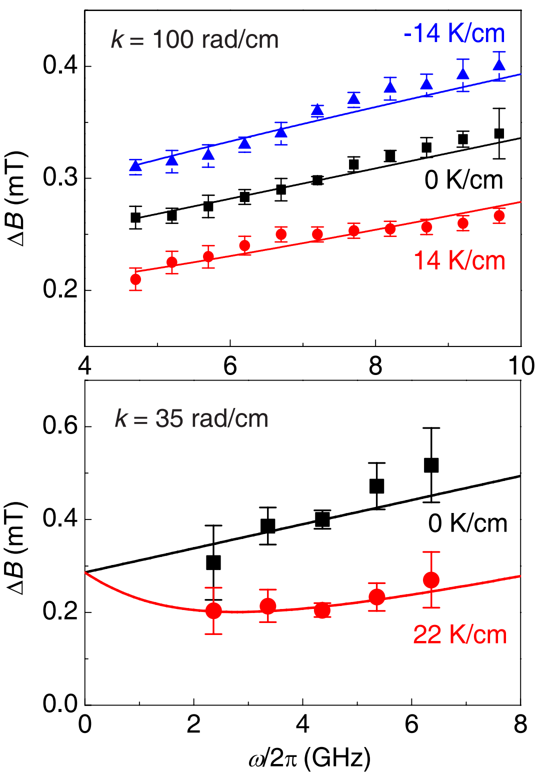

FIG. 3. Linewidth as a function of frequency at a set temperature gradient, using microprobe (top), or metal contacts (bottom) for excitation. Wavevector based on HFSS calculation. The applied temperature gradients are indicated in the figure. Top : black line yields $\alpha = 3.15\times10^{-4}$, red and blue lines using Eq. (5). Bottom : black line yields $\alpha = 6.30 \times 10^{-4}$, red line using Eq. (5). The error bars indicate the noise level.

Finally, we note that the thermal spin torque (Eq. (2) and (3)) can be expressed in terms of a spin current. To first-order in the linear response, the thermal spin torque is given by [25],

$$\boldsymbol{\tau}_{\mathrm{TST}} = \boldsymbol{k}_{\mathrm{T}} \cdot \mathrm{j_s} \tag{6}$$

where the dot stands for the tensor contraction and the thermal spin current tensor $\mathrm{j_s}$ is defined by,

$$\mathrm{j_s} = -\,\mu_0\, \boldsymbol{M}_{\mathrm{S}} \times \boldsymbol{\nabla}^{-1}\, \boldsymbol{m}_{\mathrm{k}} \tag{7}$$

The spin current density tensor $\mathrm{j_s}$ has physical dimensions ($\mathrm{J/m^2}$ in SI units) that correspond to the product of a spin density and a phase velocity. Expression (7) has the same geometry to first order as the spin-wave spin current tensor derived by Saitoh and Ando [28]. However, the physical origin of this spin current tensor is different since here, it is obtained specifically for the case of a spin current induced by a thermal gradient.

Very recently, self-oscillation based on spin orbit torque were found in YIG/Pt pillar [29] and in permalloy/Pt nanowires [30]. By analogy, we may expect self-oscillation driven by a thermal spin torque as well.

In conclusion, we have prepared thin-film YIG microstrips and found that the linewidth of transmission spectra can be broadened or narrowed by applying a thermal gradient. These observations are accounted for by an effective damping that is due to a thermal spin torque. A comprehensive theoretical analysis provides an explicit expression for this torque, which is derived from an extension of the variational principle on which the Landau-Lifshitz equation is based. This study points to the possibility of damping control in magnonic devices using a local thermal gradient.

We wish to acknowledge the support by NSF China under Grant No. 11674020 and 11444005, for S.T. by the Sino-Swiss Science and Technology Cooperation SSSTC Grant no.EG 01-032015, for F.A.V and P.C. by the Polish-Swiss Research Program NANOSPIN PSRP-045/2010, for H.Y. by the Deutsche Forschungsgemeinschaft SPP 1538 (SpinCat) grant no. AN762/1, and by the Program of Introducing Talents of Discipline to Universities in China “111 Programme” No. B16001. The authors thank Vincent Cros for comments on the manuscript.

* haiming.yu@buaa.edu.cn
† jean-philippe.ansermet@epfl.ch

[1] M. N. Baibich *et al.*, Phys. Rev. Lett. **61**, 2472 (1988).

[2] G. Binasch, P. Grünberg, F. Saurenbach, and W. Zinn, Phys. Rev. B **39**, 4828 (1989).

[3] J.C. Slonczewski, J. Magn. Magn. Mater. **159**, L1 – L7 (1996).

[4] L. Berger, Phys. Rev. B **54**, 9353–9358 (1996).

[5] A. D. Kent and D. C. Worledge, Nat. Nanotechnol. **10**, 187–191 (2015).

[6] M. Hatami, G. E. W. Bauer, Q. Zhang, and P. J. Kelly, Phys. Rev. Lett. **99**, 066603 (2007)

[7] H. Yu, S. Granville, D. P. Yu, and J.-P. Ansermet, Phys. Rev. Lett. **104**, 146601 (2010).

[8] J. C. Slonczewski, Phys. Rev. B **82**, 054403 (2010).

[9] S. D. Brechet, F. A. Vetro, E. Papa, S. E. Barnes, and J.-P. Ansermet, Phys. Rev. Lett. **111**, 087205 (2013).

[10] G. E. Bauer, E. Saitoh, and B. J. van Wees, Nat. Mater. **11,** 391–399 (2012).

[11] L. Piraux, A. Fert, P. Schroeder, R. Loloee, and P. Etienne, J. Magn. Magn. Mater. **110**, L247–L253 (1992).

[12] J. Flipse, F. Bakker, A. Slachter, F. Dejene, and B. J. Van Wees, Nat. Nanotechnol. **7**, 166–168 (2012).

[13] K. Uchida *et al.*, Nature (London) **455**, 778–781 (2008).

[14] C. Jaworski, R. Myers, E. Johnston-Halperin, and J. Heremans, Nature (London) **487**,210–213 (2012).

[15] A. Slachter, F. L. Bakker, J.-P. Adam, and B. J. van Wees, Nat. Phys. **6**, 879–882 (2010).

[16] B. Obry, V. I. Vasyuchka, A. V. Chumak, A. A. Serga, and B. Hillebrands, Appl. Phys. Lett. **101**, 192406 (2012).

[17] G. da Silva, L. Vilela-Leao, S. Rezende, and A. Azevedo, Appl. Phys. Lett. **102**, 012401 (2013).

[18] L. Lu, Y. Sun, M. Jantz, and M. Wu, Phys. Rev. Lett. **108**, 257202 (2012).

[19] A. Pushp *et al.*, Proc. Natl. Acad. Sci. U. S. A. **112**, 6585–6590 (2015).

[20] G.-M. Choi, C.-H. Moon, B.-C. Min, K.-J. Lee, and D. G. Cahill, Nat. Phys. **11**, 576–581 (2015).

[21] N. Mojumder, D. Abraham, K. Roy, and D. Worledge, IEEE Trans. Magn. **48**, 2016–2024 (2012).

[22] O. d′Allivy Kelly *et al.*, Appl. Phys. Lett. **103**, 082408 (2013).

[23] E. Papa, S. Barnes, and J.-P. Ansermet, IEEE Trans. Magn. **112**, 17006 (2015).

[24] S. D. Brechet and J.-P. Ansermet, EPL **112**, 17006 (2015).

[25] See Supplemental Material at http://link.aps.org/supplemental/..., which includes Refs. [26, 27], for additional details on theoretical derivation, sample fabrication, measurement technique, isothermal measurements and HFSS simulations.

[26] A. G. Gurevich and G. A. Melkov, *Magnetization oscillations and waves* (CRC press, 1996).

[27] D. C. Ralph and M. D. Stiles, J. Magn. Magn. Mater. **320**, 1190 (2008).

[28] D. C. Maekawa, S. O. Valenzuela, E. Saitoh, and T. Kimura, *Spin current* (Oxford University Press, 1996).

[29] M. Collet *et al.*, Nat. Commun. **7**, 10377 (2012).

[30] Z. Duan *et al.*, Nat. Commun. **5**, 5616 (2014).